

Decay of 83-min  $^{139}\text{Ba}$  to levels of  $^{139}\text{La}$  and the decay of 18-min  $^{141}\text{Ba}$  to levels of  $^{141}\text{La}$ 

Scott H. Faller, Craig A. Stone, John D. Robertson, Chien Chung,\* Namik K. Aras,<sup>†</sup> and William B. Walters  
*Department of Chemistry, University of Maryland, College Park, Maryland 20742*

R. L. Gill and A. Piotrowski<sup>‡</sup>

*Physics Department, Brookhaven National Laboratory, Upton, New York 11973*

(Received 6 March 1986)

The level structures of odd proton  $^{139}\text{La}$  and  $^{141}\text{La}$  have been studied in  $\gamma$ -ray singles, Compton-suppressed singles, coincidence, and angular correlation experiments. No evidence was observed to support the existence of any levels in  $^{139}\text{La}$  in the gap between the 166-keV  $d_{5/2}$  level and the 1209-keV  $\frac{1}{2}^+$  level, even though data were accumulated long enough to observe indirect feeding of the  $\frac{1}{2}^+$  level. Additional spin and parity assignments are suggested for a number of levels in  $^{141}\text{La}$  based on angular correlation measurements.

## I. INTRODUCTION

Recent studies<sup>1</sup> of the structure of odd-odd La and odd-odd  $N=83$  nuclides have been interpreted using the parabolic multiplet model proposed by Paar.<sup>2</sup> Central to the interpretation of the structure of odd-odd nuclides is the underlying structure of the adjacent odd-even nuclides. The multiplet fits in  $^{140}\text{La}$  were less satisfactory than those for the higher mass  $N=83$  nuclides. One source of uncertainty in the fits has to do with how well the underlying structure of odd-mass  $^{139}\text{La}$  is known<sup>3-12</sup> A second uncertainty arises from the dependence of the multiplet splitting on the difference between the occupancy  $V^2$  and the emptiness  $U^2$ , both in  $^{140}\text{La}$  and  $^{142}\text{La}$ . As transfer reactions are not available to populate the levels of  $^{141}\text{La}$ , estimates must be derived from other sources. However, almost no spin and parity assignments<sup>13-15</sup> are available for the apparently well established low-lying levels of  $^{141}\text{La}$ , the underlying odd  $Z$  nuclide for  $^{142}\text{La}$ . In this paper we report the results of a new study of the  $\gamma$ -ray spectrum of  $^{139}\text{Ba}$  decay to  $^{139}\text{La}$  levels aimed at seeking evidence for a number of proposed levels in  $^{139}\text{La}$  lying between 500 and 1200 keV. We also report the results of an on-line angular correlation study of the  $\gamma$  rays following the decay of  $^{141}\text{Ba}$  to levels of  $^{141}\text{La}$ . We propose several changes in the level scheme of  $^{141}\text{La}$  as well as a number of new spin and parity assignments.

## II. EXPERIMENTAL PROCEDURES AND RESULTS

### A. $^{139}\text{Ba}$ studies

The sources of 83-min  $^{139}\text{Ba}$  were produced by irradiating high purity  $\text{BaCO}_3$  in the National Bureau of Standards reactor. Samples containing 10 mg of barium were irradiated for 30 min at a flux of  $10^{13}$  n/cm<sup>2</sup>sec in the section of the reactor with the lowest fraction of non-thermal neutrons. The samples were dissolved in 0.1N HCl and the solution neutralized with  $\text{NH}_4\text{OH}$ . The Ba was then precipitated as  $\text{BaCrO}_4$  using a procedure

described by Sunderman and Townley.<sup>16</sup>

The decay scheme of  $^{139}\text{Ba}$ , essentially as published by Berzins, Bunker, and Starner,<sup>3</sup> is shown in Fig. 1. Approximately 99.6% of the  $\beta$  decay populates the two lower levels, with over 80% of the remainder populating the 1420-keV level. The other 0.06% populates a number of levels between 1200 and 2100 keV. The region of the  $\gamma$ -ray spectrum between 166 and 1200 keV is dominated by Compton events associated with the  $\gamma$  rays above 1200 keV. To search for very weak transitions in this region, the samples were counted with a 100-cm<sup>3</sup> Ge(Li) detector situated inside a 25 $\times$ 37 cm split-annulus Compton-suppression system.<sup>17</sup> A graded Pb-Cu absorber was used to absorb a significant fraction of the 166-keV  $\gamma$  rays. This made it possible to place the sample closer to the detector to achieve higher geometry for the higher-energy  $\gamma$  rays while maintaining a reasonable dead time in the counting system. Each sample was counted for 90 min and set aside for later counting to identify long-lived nuclides that were not entirely removed in the chemical separation. As we were primarily concerned with the energy region up to 1200 keV, high gain was used, and our spectra ranged only up to 1600 keV. With these techniques we achieved sufficient sensitivity to observe the 1053-keV  $\gamma$  ray as shown in Fig. 2, which Berzins *et al.*<sup>3</sup> could barely discern in coincidence spectra, as well as a much weaker 1043-keV  $\gamma$  ray.

In Fig. 3 are shown the level structures of  $^{139}\text{La}$  proposed by earlier investigators. As can be seen, the most serious disagreements concern the possible existence of levels at 570, 800, 830, and 1070 keV. Gamma rays from these levels populating the ground and 166-keV levels would lie at 405, 535, 565, 570, 800, 830, 905, and 1070 keV. The spin and parity<sup>18</sup> of the parent  $^{139}\text{Ba}$  are  $\frac{7}{2}^-$ . Direct  $\beta$  population of  $\frac{5}{2}^+$ ,  $\frac{7}{2}^+$ , and  $\frac{9}{2}^+$  levels can be expected by first-forbidden transitions, while population of  $\frac{3}{2}^+$  and  $\frac{11}{2}^+$  levels could be populated by first-forbidden unique  $\beta$  transitions. Population of the known  $\frac{1}{2}^+$  level at 1209 keV (Ref. 11) could occur by  $\gamma$ -ray branching from higher levels or by third-forbidden  $\beta$  decay. We

counted enough samples to observe the appearance, albeit quite weak, of the 1043-keV  $\gamma$  ray transition from the 1209-keV level to the 166-keV level. We reasoned that if the 1209-keV level were populated, then population of lower-lying  $\frac{1}{2}^-$  and  $\frac{3}{2}^-$  should have occurred even more strongly owing to the  $E^3$  and  $E^5$  energy dependence for population from whatever levels feed the 1209-keV level.

We are able to account for all of the  $\gamma$  rays observed in our spectra on the basis of known transitions in the decay of  $^{131}\text{Ba}$ ,  $^{137}\text{Ba}$ , and  $^{139}\text{Ba}$  as well as  $^{56}\text{Mn}$  and  $^{116}\text{In}^{m1}$  not completely removed in the chemical separations. As the most frequently proposed levels in the gap between 166 and 1200 keV lie near 800 keV, the portion of the spectrum between 800 and 950 keV is shown in Fig. 4. The peak at 818 keV is attributed to 54-min  $^{116}\text{In}^{m1}$  as we see other peaks associated with this activity. The peak at 847 keV is attributed to 2.6-h  $^{56}\text{Mn}$  decay, and the other peaks

associated with  $^{56}\text{Mn}$  decay are observed elsewhere.<sup>19</sup> The peak at 909 keV arises from the single escape of annihilation radiation produced by the dominant 1420-keV  $\gamma$  ray.

The peaks at 832 and 924 keV shown in Fig. 4 are well established as belonging to the decay of 11-day  $^{131}\text{Ba}$  and are observed in approximately the same ratio in the background spectrum taken the next day as shown in Fig. 5. If the intensity of the 832-keV peak resulting from the uncertainty in our measured ratio and the reported intensities of the 832- and 923-keV peaks is attributed to the decay of a level at 832 keV in  $^{139}\text{La}$ , that residual intensity would be 0.005 relative to 100 for the 1420-keV peak. This intensity would set a lower limit of 12.5 for the  $\log ft$  if the population of such an 832-keV level all came from direct  $\beta$  decay. This lower limit is already 3 orders of magnitude higher than the  $ft$  value for feeding of the  $\frac{3}{2}^+$

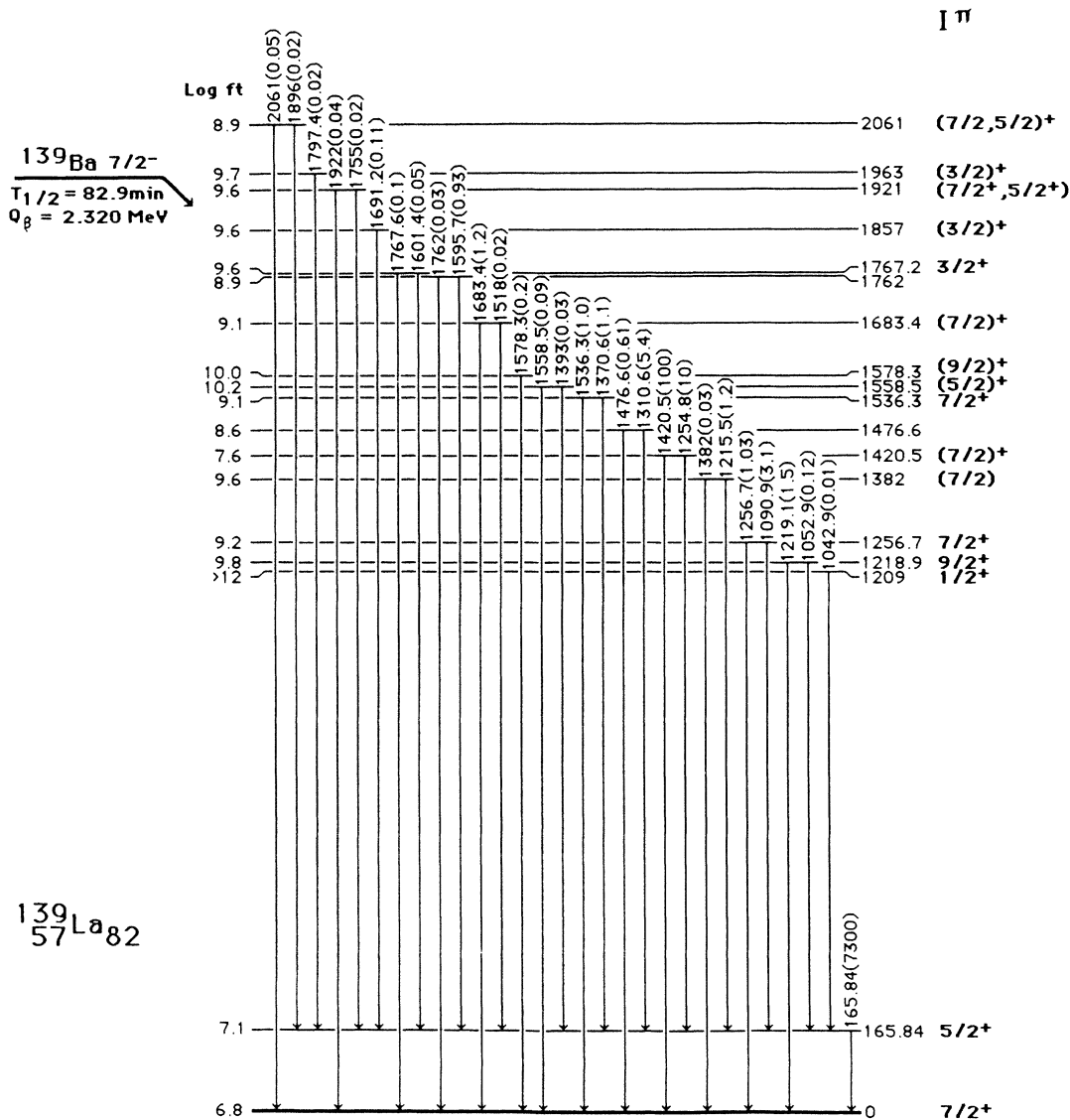


FIG. 1. Decay scheme of 82.9-min  $^{139}\text{Ba}$  to levels of  $^{139}\text{La}$  essentially as proposed by Berzins, Bunker, and Starner (Ref. 3). Additional data on weak transitions are from this work.

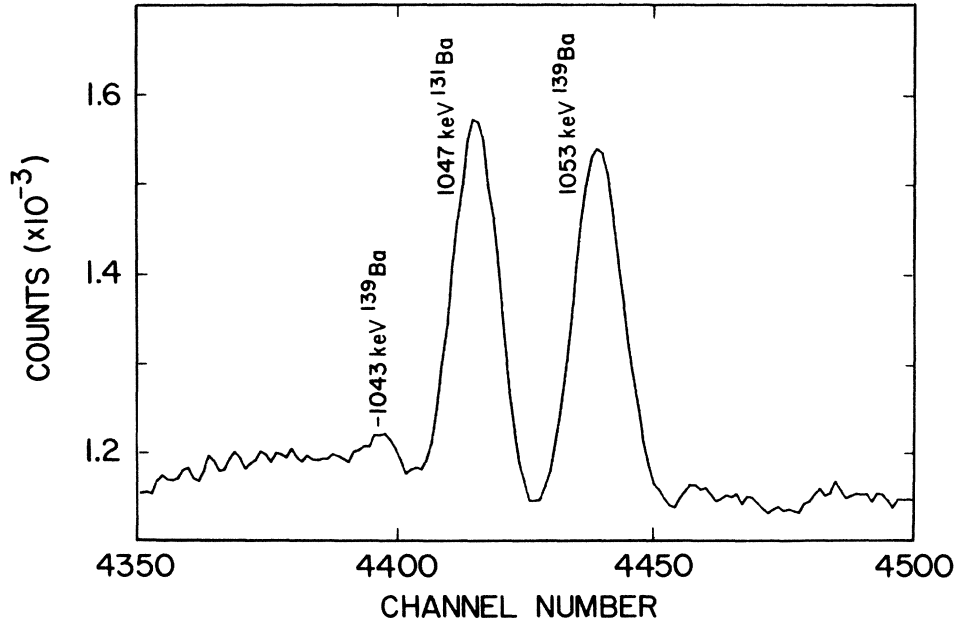


FIG. 2. Compton-suppressed  $\gamma$ -ray spectrum of  $^{139}\text{Ba}$  decay between 1000 and 1100 keV.

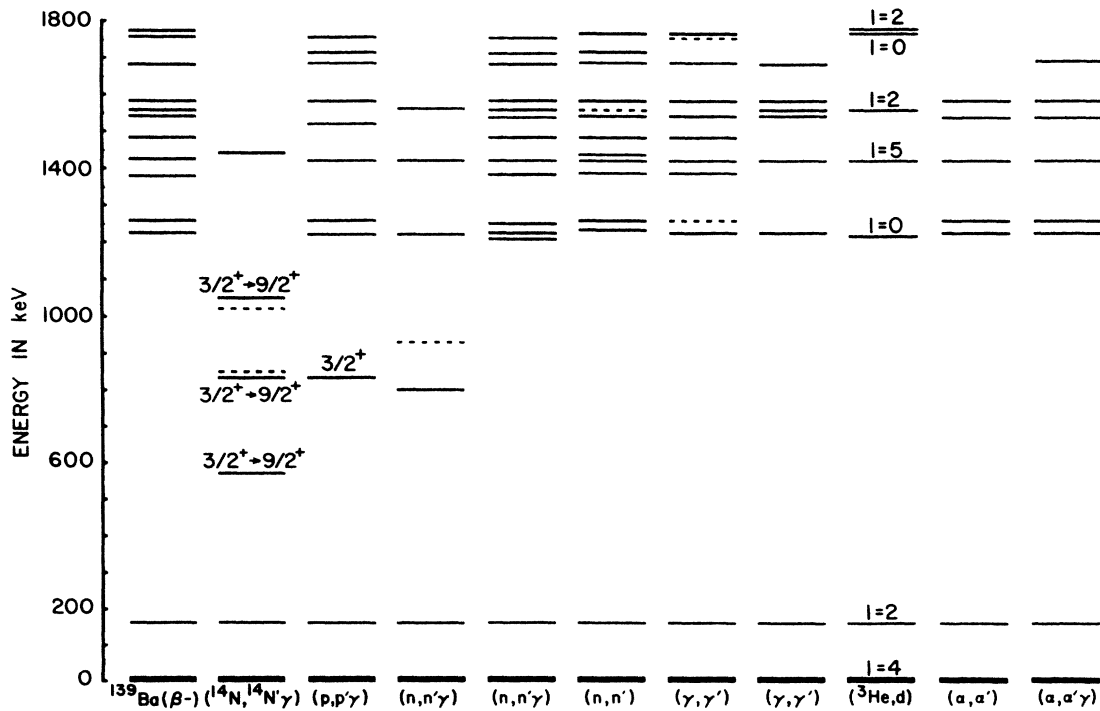


FIG. 3. Results of previous studies of the structure of  $^{139}\text{La}$ . The  $^{139}\text{Ba}$  decay data are from Ref. 3, the  $(^{14}\text{N}, ^{14}\text{N}'\gamma)$  data are from Ref. 4, the  $(p, p'\gamma)$  data are from Ref. 5, the  $(n, n'\gamma)$  data with the intermediate levels at 800 and 900 keV are from Ref. 6, the  $(n, n'\gamma)$  data with no intermediate levels are from Ref. 7, the  $(n, n')$  data are from Ref. 9, the  $(\gamma, \gamma')$  are from Refs. 9 and 10, the  $(^3\text{He}, d)$  data are from Ref. 11, and the  $(\alpha, \alpha')$  and  $(\alpha, \alpha'\gamma)$  data are from Ref. 12.

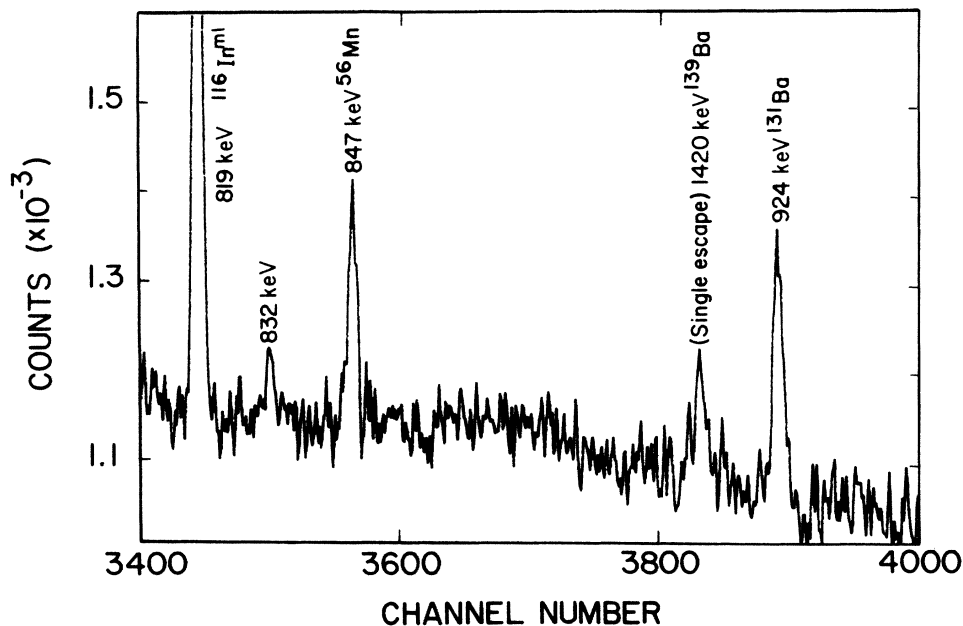


FIG. 4. Compton-suppressed  $\gamma$ -ray spectrum of  $^{139}\text{Ba}$  decay between 800 and 950 keV.

levels at 1766, 1857, and 1963 keV.

No evidence was observed for any other peaks that could feed either the ground state or the 166-keV first-excited levels from any of the proposed levels shown in Fig. 3 below 1200 keV.

#### B. $^{141}\text{La}$ studies

The angular correlation studies of the  $\gamma$  rays emitted following the decay of 18-min  $^{141}\text{Ba}$  to levels of  $^{141}\text{La}$

were carried out at the on-line mass separator facility TRISTAN located at the high-flux beam reactor at Brookhaven National Laboratory. Previous investigators have achieved considerable, but not complete, agreement as to this decay scheme and have reported both  $\gamma$ -ray and conversion-electron energy and intensity data.<sup>13-15</sup> The experimental uncertainties in the conversion-electron intensities were too large to do more than distinguish between  $E1$  and  $M1 + E2$  transitions. Thus, our primary goal was to measure angular correlations among the more

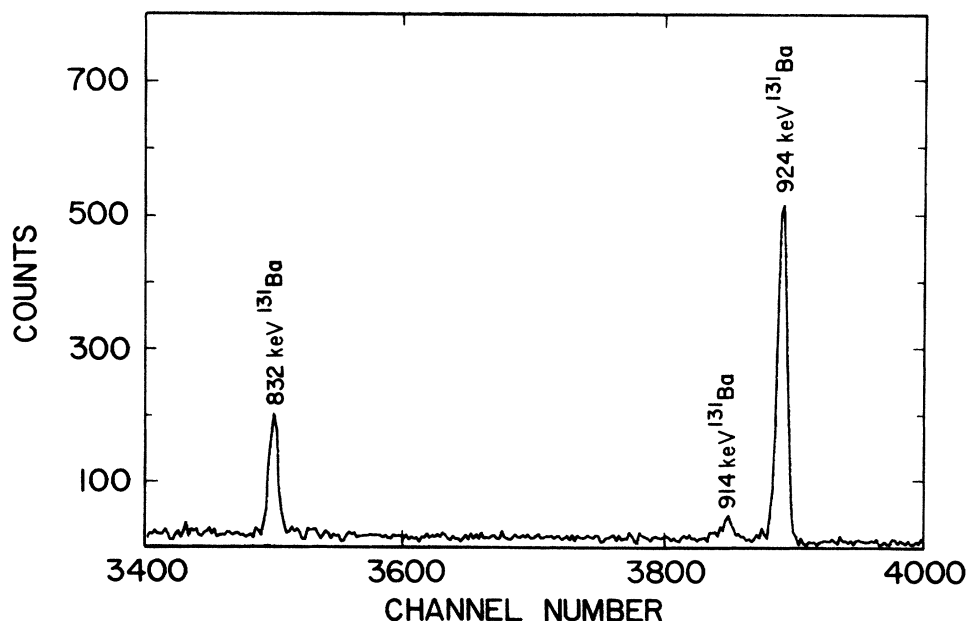


FIG. 5. Compton-suppressed  $\gamma$ -ray spectrum of  $^{139}\text{Ba}$  decay taken 24 h after irradiation showing the residual  $\gamma$  rays from  $^{131}\text{Ba}$  decay in the energy range between 800 and 950 keV.

TABLE I.  $\gamma$ -ray transitions in  $^{141}\text{Ba}$  below 2500 keV.

$E_\gamma$ (keV)	$I_\gamma$ (rel)	$\Delta I_\gamma$	$E_i$ (keV)	$E_f$ (keV)	$E_\gamma$ (keV)	$I_\gamma$ (rel)	$\Delta I_\gamma$	$E_i$ (keV)	$E_f$ (keV)
67.8	<0.05		648	580	867.8	2.4	0.4	1172	304
112.8	22	2	580	468	876.3	80	2.7	1067	190
113.9	2.3	1	304	190	880.8	0.7	0.4	1566	686
163.0	6.4	0.7	468	304	881.2	3.2	0.5	1873	992
180.8	11.2	3.5	648	468	885.2	1.0	0.2	1717	832
190.4	1000	30	190	0	909.3	2.5	0.4	1742	832
234.9	1.3	0.3	1067	832	917.4	1.2	0.2	2469	1552
242.7	2.	0.3	1172	930	929.5	16.3	0.9	930	0
277.1	509	15	468	190	943.2	17.5	0.9	1873	930
281.6	2.2	0.3	930	648	959.0	1.2	0.3		
304.4	553	17	304	0	967.6	0.7	0.2	2469	1502
321.5	0.6	0.3	1873	1552	981.2	4	1	1629	648
343.9	314	9	648	304	981.7	16	2	1172	190
349.5	5	0.4	930	580	996.8	2.8	0.5	1926	930
359.2	0.21	0.17	827	468	1008.4	1.4	0.3		
364.5	12.8	0.6	832	468	1012.5	3.2	0.5	1845	832
381.4	2.6	0.4	686	304	1034.3	4.1	0.9	1502	468
390.0	29	1	580	190	1039.9	1.9	0.3	1040	0
418.8	1.4	0.3	1067	648	1046.3	7.4	0.9	1873	827
457.8	109	3	648	190	1055.2	2.0	0.4	1742	686
462.3	106	3	930	468	1066.6	2.2	0.4		
462.9	1.2	0.6	1502	1040	1093.2	2	1	1742	648
467.5	124	4	468	0	1094.2	3	1	1926	832
486.7	1.3	0.3	1067	580	1136.8	0.8	0.2	1717	580
510.3	3	1	1502	992	1147.0	0.6	0.2		
522.3	9.4	0.3	827	304	1160.8	24	1	1629	468
524.3	10	0.4	1172	648	1173.1	3.8	0.3	1172	0
527.6	9.9	1.5	832	304	1178.3	1.5	0.3	2218	1040
541.6	1.8	0.5	2469	1926	1187.8	0.24	0.19	1873	686
551.0	2.1	0.3			1197.3	104	3	1502	304
561.7	4.1	0.5	1629	1067	1224.9	9.5	1.3	1873	648
572.3	5.7	0.5	1040	468	1236.0	4.2	0.5	1427	190
588.8	2.7	0.4	1629	1040	1264.0	19	1	1845	580
599.4	5.8	0.5	1067	468	1273.4	10.9	0.7	1742	468
609.0	8.0	0.9	1189	580	1278.0	14.4	0.8	1926	648
611.3	0.40	0.1			1302.1	2.4	0.3		
625.4	78	2	930	304	1309.4	5.1	0.7	2377	1067
636.2	6.9	0.3	827	190	1311.2	14.3	1	1502	190
641.5	8.7	0.4	832	190	1323.8	21	1	1629	304
648.1	137	4	648	0	1345.7	3.9	0.4	1926	580
655.3	0.4	0.3			1354.6	1.6	0.2		
670.3	4.0	0.4	1502	832	1357.1	2.3	0.3		
675.4	6.6	0.6	1502	827	1361.2	0.7	0.25	1552	190
685.4	4	1	686	0	1376.8	18	1	1845	468
688.0	1.1	0.3	992	304	1391.0	1.2	0.3	2218	827
698.8	8.7	5	1629	930	1405.1	7.1	0.5	1873	468
700.7	2.8	0.3	1873	1172	1436.6	18.8	1.2	1742	304
704.8	5.8	0.6	1172	468	1437.8	4.2	0.8	1629	190
739.2	105	3	930	190	1447.0	3.1	0.4	2377	930
753.8	1.0	0.4	1926	1172	1455.9	2.8	0.7	2386	930
762.0	4.2	0.6	1067	304	1460.0	16.6	1.5	1926	468
778.4	1.7	0.4	1427	648	1501.4	8.5	1.3	1502	0
801.7	2.9	0.4	992	190	1540.2	1.8	0.2		
805.3	1.4	0.3	1845	1040	1547.1	0.7	0.2		
806.4	1.4	0.3	1873	1067	1550.2	8.5	0.5	1742	190
826.4	8.6	0.5	827	0	1568.3	6.1	0.6	1873	304
831.7	35.1	1.7	832	0	1569.8	1.0	0.5	2218	648
833.8	3.6	0.8	1873	1040	1600.6	1.4	0.3	2181	580
841.0	1.0	0.2	2469	1629	1609.3	0.9	0.2	2441	832
846.6	1.4	0.2	1427	580	1621.4	1.5	0.4	1926	304

TABLE I. (Continued).

$E_\gamma$ (keV)	$I_\gamma$ (rel)	$\Delta I_\gamma$	$E_i$ (keV)	$E_f$ (keV)	$E_\gamma$ (keV)	$I_\gamma$ (rel)	$\Delta I_\gamma$	$E_i$ (keV)	$E_f$ (keV)
1642.5	1.8	0.3	2469	827	1912.2	3.3	0.5		
1653.6	20	1	1845	190	1918.3	1.3	0.2		
1682.3	37	2	1873	190	1990.0	5.4	1.0		
1712.7	4.6	0.8	2293	580	2026.2	9.8	1.5		
1727.7	2.0	0.2			2136.6	0.7	0.2		
1735.4	4.6	0.8			2164.0	3.9	0.9		
1740.6	7.1	0.6			2195.0	2.1	0.3		
1795.4	12.5	0.9			2277.9	2.4	0.2		
1820.5	2.6	0.3			2468.8	5.3	0.3		
1859.9	2.0	0.3							

intense cascades to determine spins and parities.

The general description of the TRISTAN facility and the operation of the four-detector coincidence and angular correlation system have been described in earlier publications.<sup>20,21</sup> For this experiment, a positive surface ionization source with a target of enriched  $^{235}\text{U}$  and  $\text{UO}_2$  in a solid graphite matrix was used. The source was situated in an external beam in a flux of  $2 \times 10^{10}$  n/cm<sup>2</sup>sec and maintained at a 50 kV potential. The accelerated positive ions were implanted in an aluminized mylar tape that could be moved, when an appropriate sample had been collected, to a position centered with respect to four large volume ( $> 75$  cm<sup>3</sup>) Ge detectors having full-width at half-maximum values of  $< 2.0$  keV for 1.33 MeV  $\gamma$  rays. The detectors were located at a distance of 7.6 cm from the source, and the energy range spanned by the amplifiers was from 20 to 2000 keV. The detectors were located at 55, 90, and 180 degrees relative to the first detector, giving angular correlation data at 90, 125, 145, and 180 degrees. The data were normalized using singles spectra gated with the same constant-fraction discriminator used to trigger the coincidence system, and by measuring the angular correlations of  $\gamma$  rays in  $^{140}\text{Ba}$  following the decay of  $^{140}\text{Cs}$ . Mass contamination and background were determined by collecting a series of 32 time-sequential 8192-channel spectra after each move of the tape.

In Table I are shown the energies, intensities, and placements for the  $\gamma$  rays that we observe below 2.5 MeV. The proposed decay scheme incorporating our new data is shown in Fig. 6 for levels below 2 MeV. We corroborate levels at 1040, 1427, and 1566 keV proposed by Lee and Talbert<sup>13</sup> but not observed by Proto *et al.*,<sup>14</sup> and we propose two additional levels at 1552 and 1717 keV.

The proposed placement of a level at 1552 keV is supported by coincidence between the 1361-keV  $\gamma$  ray and both the 321-keV  $\gamma$  ray and the 917-keV  $\gamma$  ray (which depopulates a level of 2439-keV not shown in Fig. 6). The proposed placement of a level at 1717 keV is supported by coincidences between  $\gamma$  rays at 885 and 832 keV, the absence of coincidences between the 885- and 302-keV  $\gamma$  rays, and by coincidences between the 390- and 1137-keV  $\gamma$  rays. The possible placement of a level at 1138 keV proposed by Proto *et al.*<sup>14</sup> was not supported, as the 670-keV  $\gamma$  ray was found to populate the 832-keV level and no evidence for a 310-keV  $\gamma$  ray was found.

The  $\beta$ -branching and  $\log ft$  values were computed using

our intensity values for  $\gamma$  rays with energies below 2 MeV and the intensities of Lee and Talbert<sup>13</sup> for  $\gamma$  rays above 2 MeV. Angular correlation data were analyzed for 11 intense cascades. The resulting data were fit to the function

$$W(\theta) = A_0[1 + A_2 P_2(\cos\theta) + A_4 P_4(\cos\theta)]$$

in order to determine the best values for the  $A_2$  and  $A_4$  coefficients for each cascade. The data were also fit with only  $A_2$  allowed to vary. The resulting values are listed in Table II.

### C. Spin and parity assignments in $^{141}\text{La}$

The preponderance of experimental data support spin and parity of  $\frac{3}{2}^-$  for the ground state of  $^{141}\text{Ba}$ , although only the  $\frac{3}{2}$  spin value has been measured.<sup>22</sup> Systematic evidence for a  $\frac{7}{2}^+$  ground state and a  $\frac{5}{2}^+$  first excited state in  $^{141}\text{La}$  is obtained from the well established level structure of  $^{139}\text{La}$ . The weak  $\beta$  decay from  $^{141}\text{Ba}$  to the ground state of  $^{141}\text{La}$  is consistent with a first-forbidden unique  $\beta$  transition and a  $\frac{7}{2}^+$  spin and parity for the ground state of  $^{141}\text{La}$ . Moreover, the decay of  $^{141}\text{La}$  to the  $\frac{7}{2}^-$  ground state and  $\frac{9}{2}^-$  level at 1354 keV in  $^{141}\text{Ce}$  sets a lower limit of  $\frac{7}{2}$  for the spin of the  $^{141}\text{La}$  ground state. The  $M1 + E2$  multipolarity of the 190-keV transition measured by Proto *et al.*<sup>14</sup> and the strong  $\beta$  feeding of the 190-keV level limit its spin and parity to  $\frac{3}{2}^+$  or  $\frac{5}{2}^+$ . The angular correlations for several strong cascades are shown in Figs. 7 and 8. The  $A_2$  value of  $0.19 \pm 0.03$  for the 457-190-keV cascade is well above the largest value possible for either a  $\frac{3}{2}(M1/E2)\frac{3}{2}(E2)\frac{7}{2}$  ( $\sim 0.09$ ) or  $\frac{5}{2}(M1/E2)\frac{3}{2}(E2)\frac{7}{2}$  ( $\sim 0.11$ ) cascade, thereby ruling out the  $\frac{3}{2}^+$  possibility. Thus,  $\frac{5}{2}^+$  spin and parity are established for the 190-keV level in  $^{141}\text{La}$ .

The 304-keV level decays by an  $M1 + E2$  transition to the  $\frac{7}{2}^+$  ground state and is not significantly fed in  $\beta$  decay, limiting its spin to a range from  $\frac{3}{2}^+$  to  $\frac{11}{2}^+$ . The 344-304-keV cascade from the strongly  $\beta$ -fed level at 648 keV shows definite  $A_4$  character (as seen in Fig. 7) which eliminates the  $\frac{3}{2}^+$  possibility. The fact that this level is populated by the  $\gamma$  decay of nearly every excited level that populates the  $\frac{5}{2}^+$  190-keV level strongly suggests  $\frac{5}{2}^+$  spin and parity for the 304-keV level.

The 467-keV level is limited to spin and parity assign-

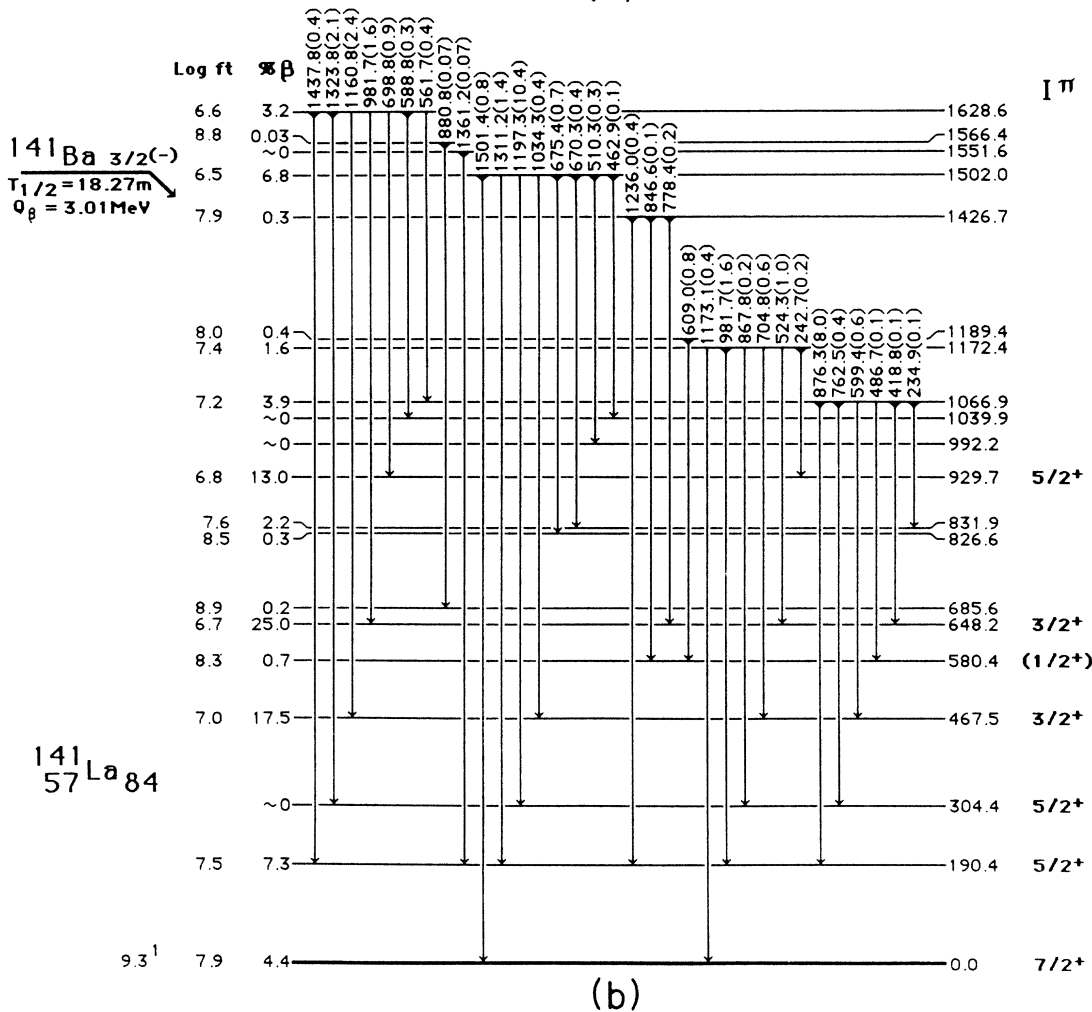
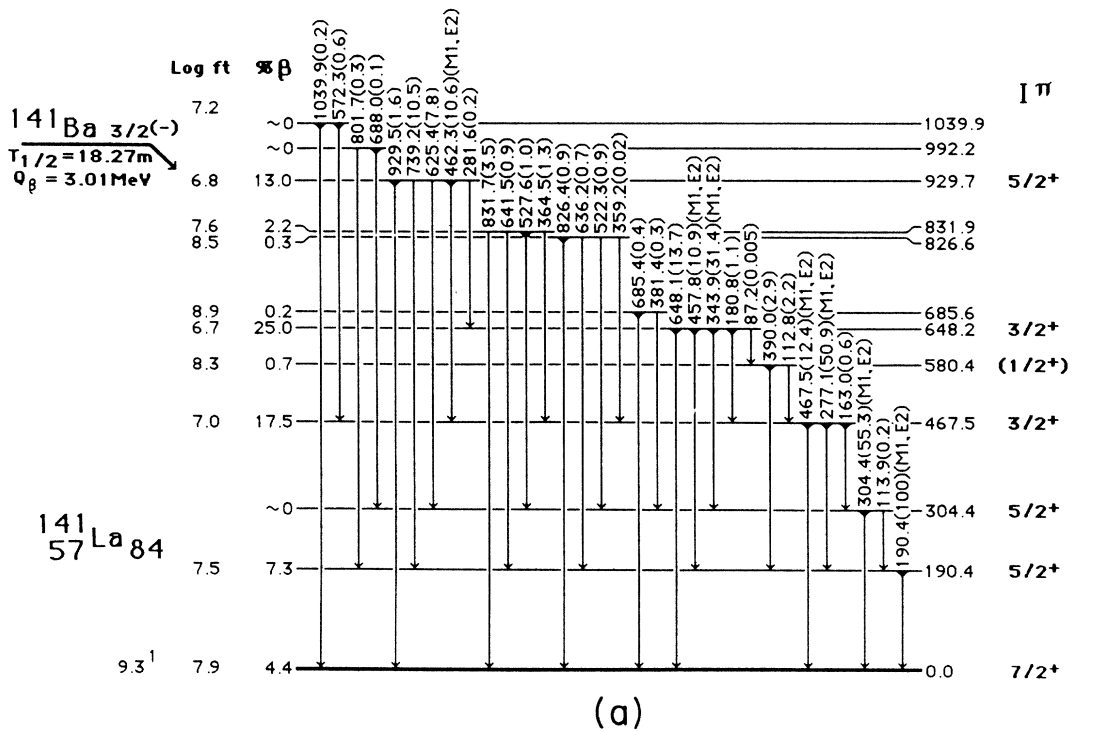


FIG. 6. (a) Decay scheme of  $^{141}\text{Ba}$  to levels of  $^{141}\text{La}$  up to 1050 keV. (b) Decay scheme of  $^{141}\text{Ba}$  to levels of  $^{141}\text{La}$  between 1050 and 1650 keV. (c) Decay scheme of  $^{141}\text{Ba}$  to levels of  $^{141}\text{La}$  between 1650 and 2000 keV.

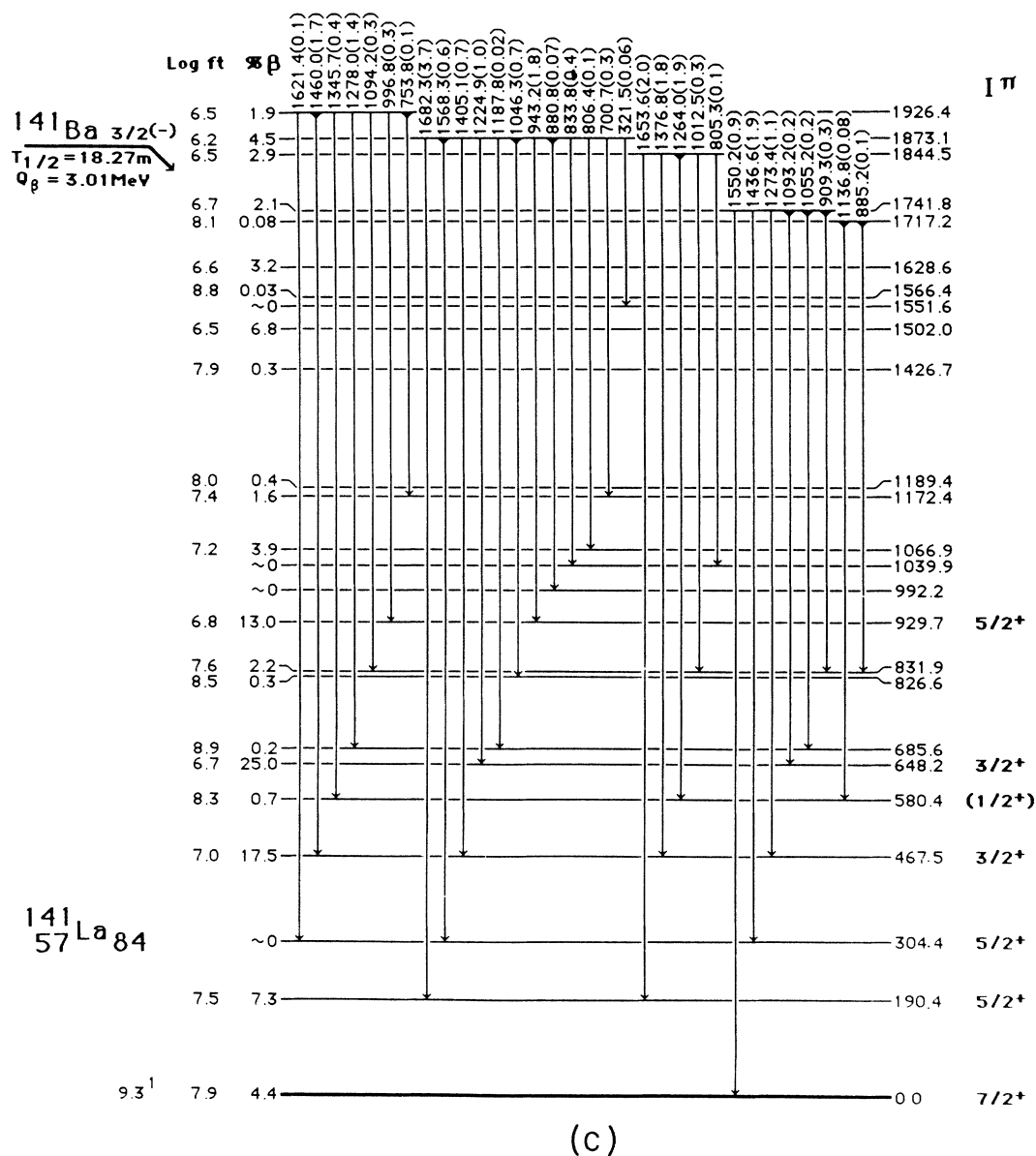


FIG. 6. (Continued).

TABLE II. Angular correlation fits for  $^{141}\text{La}$ .

$\gamma$ -ray cascade (keV)	$A_2$	Error	$A_4$	Error	$A_2^a$	Error
277-190	0.12	0.02	0.061	0.011	0.12	0.03
390-190	-0.011	0.04	0.0084	0.0540	-0.099	0.024
457-190	0.19	0.03	0.029	0.017	0.18	0.03
739-190	0.043	0.015	-0.023	0.019	0.038	0.015
876-190	0.088	0.017	-0.120	0.040	0.070	0.017
180-277	-0.13	0.10	0.051	0.130	-0.12	0.05
364-277	-0.038	0.096	0.030	0.120	-0.033	0.045
163-304	-0.034	0.100	0.038	0.132	-0.029	0.050
343-304	-0.11	0.01	0.073	0.013	-0.10	0.01
625-304	0.017	0.019	-0.059	0.026	-0.012	0.019
1197-304	0.12	0.03	-0.10	0.04	0.13	0.03

<sup>a</sup>Data fitted with no  $A_4$  coefficient.



ments of  $\frac{3}{2}^+$  or  $\frac{5}{2}^+$  by the strong  $\beta$  feeding, the  $\gamma$  transition to the  $\frac{7}{2}^+$  ground state, and the conversion coefficient<sup>14</sup> for the 277-keV transition which allows  $M1$ ,  $E2$ , or  $M1+E2$  multipolarity. The 277-190-keV cascade from this level is the strongest in this decay scheme. The positive sign for both  $A_2$  and  $A_4$  eliminate the  $\frac{5}{2}^+$  possibility, leaving  $\frac{3}{2}^+$  as the only choice. Moreover,  $A_4$  values for the two cascades through this level are well within  $1\sigma$  of the zero value required by a  $\frac{3}{2}^+$  assignment.

The 580-keV level is the only low-lying level that does not have a  $\gamma$ -ray branch to the  $\frac{7}{2}^+$  ground state and is therefore the only low-lying level that can be assigned  $\frac{1}{2}^+$ . The angular correlation of the weak 390-190-keV  $\gamma$ -ray cascade is consistent with a  $\frac{1}{2}(E2)\frac{5}{2}(M1+\delta^2E2)\frac{7}{2}$  cascade having a  $\delta$  value confined to the range determined from the 277-190-keV cascade. We show a tentative  $\frac{1}{2}^+$  assignment for this level in Fig. 6.

The 648- and 930-keV levels are limited to  $\frac{3}{2}^+$  and  $\frac{5}{2}^+$  by the strong population of these levels in  $\beta$  decay, a  $\gamma$ -ray branch to the ground state, and by  $M1+E2$  transitions to lower-lying positive parity levels. The positive  $A_4$  value obtained from the fit of the 458-190-keV and 344-304-keV cascades require the 648-keV level to have a  $\frac{3}{2}$  spin, while the negative  $A_4$  value for the 739-190 keV and 625-304 keV cascades clearly indicate a  $\frac{5}{2}$  spin assignment for the 930-keV level.

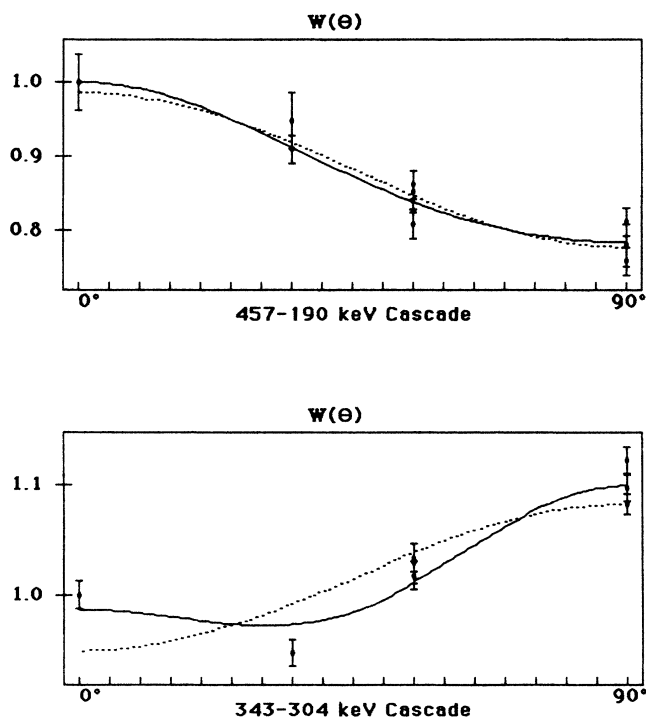


FIG. 7. Angular correlation data for the 457-190-keV and 304-343-keV cascades. The dashed line is the parametric fit for  $A_4=0$  and the solid line is the fit where  $A_2$  and  $A_4$  were both allowed to vary.

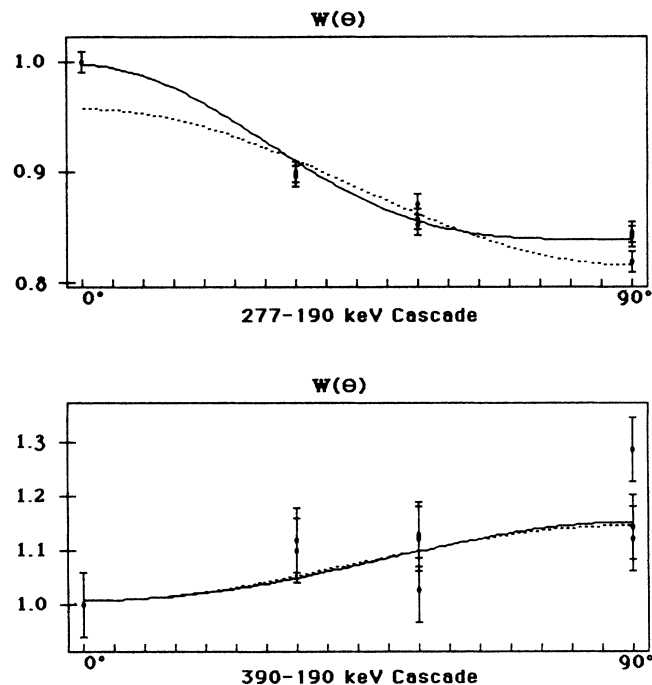


FIG. 8. Angular correlation data for the 277-190- and 390-190-keV cascades. The dashed line is the parametric fit for  $A_4=0$  and the solid line is the fit where  $A_2$  and  $A_4$  were both allowed to vary.

### III. DISCUSSION

The levels of the odd- $Z$   $N=82$  isotopes with  $50 < Z < 68$  are shown<sup>23-40</sup> in Fig. 9. From  $Z=51-63$ , the lowest two levels are the single-particle  $g_{7/2}$  and  $d_{5/2}$  orbitals, with the former being the ground state until filled by eight protons and the latter the ground state until the subshell closure is reached. The failure to find any evidence for levels in  $^{139}\text{La}$  in the gap between the 166- and 1290-keV levels removes one uncertainty in the interpretation of the levels of  $^{140}\text{La}$ . In particular, it is not possible to suggest that the levels in the 500-800-keV range in  $^{140}\text{La}$  are perturbed by multiplets associated with levels in  $^{139}\text{La}$  in this energy range.

The absence of levels in this gap also has implications about the occupancies in the odd- $Z$   $N=82$  isotones. At higher energies there is a group of core coupled levels whose lowest member lies within 300 keV of the energy of the  $2^+$  level in the core nucleus. The additional low-lying  $\frac{5}{2}^+$  level that is observed only in  $^{135}\text{I}$  and  $^{137}\text{Cs}$  is thought to arise from a  $(g_{7/2})^3$  configuration. These states have been described in a number of different cluster and shell model calculations.<sup>41-43</sup> As at least three particles or three holes in the  $g_{7/2}$  orbital are required for such an additional level, the absence of a second low-lying  $\frac{5}{2}^+$  level in  $^{139}\text{La}$  can be attributed to the combination of the high occupancy of the  $g_{7/2}$  orbital and the energy required to lift a pair of protons from the  $g_{7/2}$  orbital to the  $d_{5/2}$  orbital. Occupancy values<sup>44-46</sup> have been calculated by several investigators as a part of proton transfer studies of



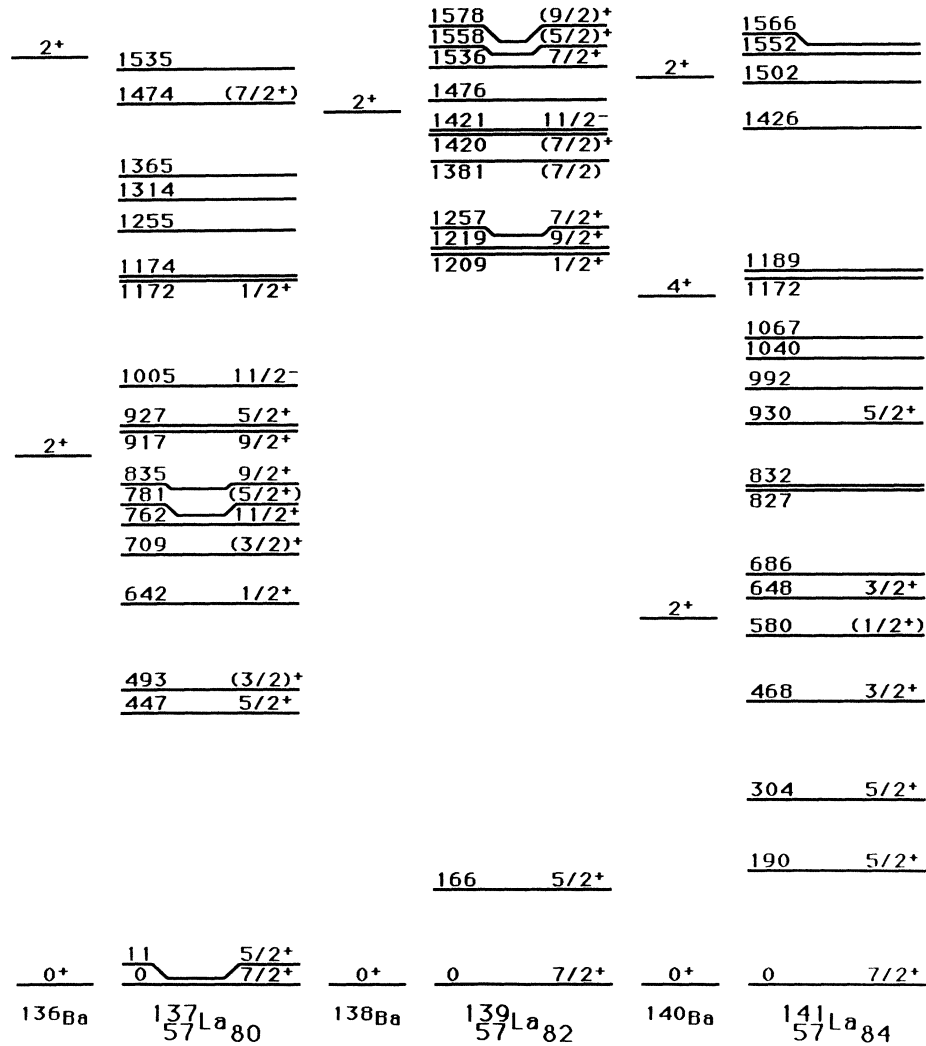


FIG. 10. Level systematics for the low-lying levels of the La isotopes with  $N = 80, 82,$  and  $84$ . The data for  $^{137}\text{La}$  are from Ref. 47.

split between the  $\frac{5}{2}^+$  levels in  $^{137}\text{La}$  can be attributed to the noticeably higher energy of the  $2^+$  core level in  $^{136}\text{Ba}$  relative to  $^{140}\text{Ba}$ . Orbital occupancy is governed by the interplay of pairing strength  $G$  and distance between single particle levels  $\rho^{-1}$  with the increased relative pairing interaction tending to smooth out the occupancy.<sup>48</sup> The smoother occupancy values in  $^{141}\text{La}$  translate directly into a prediction of less splitting of the multiplets in odd-odd  $^{142}\text{La}$ , as  $U^2 - V^2$  will be nearer zero for both the  $g_{7/2}$  (less filled) and  $d_{5/2}$  (more filled) orbitals.

In summary, the results of our study of the decay of  $^{139}\text{Ba}$  to levels of  $^{139}\text{La}$  support earlier Coulomb excitation, particle transfer, and radioactivity<sup>3,49,50</sup> studies that find no levels in  $^{139}\text{La}$  between the  $d_{5/2}$  level at 166 keV and the  $\frac{1}{2}^+$  level at 1209 keV. In turn, the absence of levels in this gap, particularly the absence of the second low-lying  $\frac{5}{2}^+$  level arising from a  $(g_{7/2})^3$  configuration, suggests that the seven protons in  $^{139}\text{La}$  are confined almost entirely to the  $g_{7/2}$  orbital, with little occupancy of the  $d_{5/2}$  orbital. The structure of  $^{139}\text{La}$  stands in sharp con-

trast to both  $^{137}\text{La}$  and  $^{141}\text{La}$ , which our new measurements show are quite similar. The additional low-lying  $\frac{5}{2}^+$  level in these non-closed-shell nuclides is similar to the additional low-lying  $\frac{5}{2}^+$  level in  $^{135}\text{I}$  and  $^{137}\text{Cs}$  and indicates lower occupancy of the  $g_{7/2}$  proton orbital. The interaction between valence protons and neutrons has recently been shown by Casten<sup>51</sup> to play a vital role in the collectivity of even-even nuclei. The presence of even one pair of neutrons is observed to produce a sufficient occupancy change to leave three proton holes present in  $^{137}\text{La}$  and  $^{141}\text{La}$ .

The authors wish to express their appreciation to the scientific and technical staff members of the Neutron Nuclear Physics Group at Brookhaven National Laboratory for their assistance and hospitality during the performance of these experiments and to the U.S. Department of Energy for support of this work through Contracts DE-AS05-79ER10494 and DE-AC02-76CH00016.

- \*Present address: Institute for Nuclear Science, National Tsing Hua University, Hsinchu 300, Taiwan, Republic of China.
- †Present address: Department of Chemistry, Middle East Technical University, Ankara, Turkey.
- ‡Present address: Institute for Nuclear Studies, 05-400 Otwock, Warsaw, Poland.
- <sup>1</sup>W. B. Walters, C. Chung, D. S. Brenner, A. Aprahamian, R. L. Gill, R. E. Chrien, M. Shmid, A. Wolf, and L.-J. Yuan, Phys. Lett. **125B**, 351 (1983); C. Chung, W. B. Walters, D. S. Brenner, A. Aprahamian, A. Wolf, R. L. Gill, M. Shmid, Z. Berant, R. E. Chrien, and L.-J. Yuan, Phys. Rev. C **28**, 2099 (1984).
- <sup>2</sup>V. Paar, Nucl. Phys. **A331**, 16 (1979).
- <sup>3</sup>G. Berzins, M. E. Bunker, and J. W. Starnner, Nucl. Phys. **A128**, 294 (1969).
- <sup>4</sup>D. G. Alkazov, K. I. Erokhina, and I. Kh. Lemberg, Bull. Acad. Sci. USSR, Phys. Ser. **29**, 137 (1965).
- <sup>5</sup>R. G. Kulkarni and K. Andredev, Can. J. Phys. **57**, 1940 (1979).
- <sup>6</sup>V. M. Pomanenko, S. P. Sit'ko, V. I. Strizhak, and V. A. Shevchenko, Yad. Fiz. **9**, 1129 (1969) [Sov. J. Nucl. Phys. **9**, 660 (1969)].
- <sup>7</sup>P. van der Merwe, I. V. van Heerden, W. R. McMurray, and J. G. Malan, Nucl. Phys. **A124**, 433 (1969).
- <sup>8</sup>J. G. Malan, W. R. McMurray, P. van der Merwe, I. J. van Heerden, and C. A. Engelbrecht, Nucl. Phys. **A124**, 111 (1969).
- <sup>9</sup>H. Szichman, Y. Schlesinger, G. Ben-David, and D. Pavel, Nucl. Phys. **A148**, 369 (1970).
- <sup>10</sup>W. J. Alstron III and R. G. Arnold, Bull. Am. Phys. Soc. **15**, 100 (1970).
- <sup>11</sup>B. H. Wildenthal, E. Newman, and R. L. Auble, Phys. Rev. C **3**, 1199 (1971).
- <sup>12</sup>R. Graetzer, A. C. Bouley, and G. Plesko, Nucl. Phys. **A176**, 433 (1971).
- <sup>13</sup>M. A. Lee and W. L. Talbert, Jr., Phys. Rev. C **21**, 328 (1980).
- <sup>14</sup>A. N. Proto, D. Otero, and E. Achterberg, J. Phys. G **5**, 121 (1979).
- <sup>15</sup>V. Berg, A. Høglund, and B. Fogelberg, Nucl. Phys. **A155**, 297 (1970).
- <sup>16</sup>D. N. Sunderman and C. W. Townley, *The Radiochemistry of Barium, Calcium, and Strontium* (Subcommittee on Radiochemistry, National Academy of Sciences—National Research Council, Washington, D.C., 1960).
- <sup>17</sup>D. L. Anderson, M. P. Failey, W. H. Zoller, G. E. Gordon, W. B. Walters, and R. M. Lindstrom, J. Radioanal. Chem. **63**, 97 (1981).
- <sup>18</sup>L. K. Peker, Nucl. Data Sheets (N.Y.) **32**, 1 (1981).
- <sup>19</sup>*Tables of Isotopes*, edited by C. M. Lederer and V. S. Shirley (Wiley, New York, 1978).
- <sup>20</sup>R. L. Gill, M. L. Stelts, R. E. Chrien, V. Manzella, and H. Liou, Nucl. Instrum. Methods **186**, 243 (1981).
- <sup>21</sup>A. Wolf, C. Chung, W. B. Walters, G. Peaslee, R. L. Gill, M. Schmid, V. Manzella, E. Meier, M. L. Stelts, H. I. Liou, R. E. Chrien, and D. S. Brenner, Nucl. Instrum. Methods **206**, 397 (1983).
- <sup>22</sup>A. C. Mueller, F. Buchinger, W. Klempt, E. W. Otten, R. Neugart, C. Ekstrom, and J. Heinemeier, Nucl. Phys. **A403**, 234 (1983).
- <sup>23</sup>J. Blomqvist, A. Kerek, and B. Fogelberg, Z. Phys. A **314**, 199 (1983).
- <sup>24</sup>Yu. V. Sergeev and V. M. Sigalov, Nucl. Data Sheets (N.Y.) **34**, 475 (1981).
- <sup>25</sup>M. Samri, G. J. Costa, G. Klotz, D. Magnac, R. Seltz, J. P. Zirnheld, Z. Phys. A **321**, 255 (1985).
- <sup>26</sup>W. R. Western, J. C. Hill, W. L. Talbert, Jr., W. C. Schick, Jr., Phys. Rev. C **15**, 1822 (1977).
- <sup>27</sup>L. K. Peker, Nucl. Data Sheets (N.Y.) **38**, 87 (1983).
- <sup>28</sup>L. K. Peker, Nucl. Data Sheets (N.Y.) **36**, 289 (1982).
- <sup>29</sup>L. K. Peker, Nucl. Data Sheets (N.Y.) **32**, 1 (1982).
- <sup>30</sup>L. K. Peker, Nucl. Data Sheets (N.Y.) **32**, 267 (1979).
- <sup>31</sup>H. Prade, W. Enghardt, H. V. Jager, L. Kaubler, H. J. Keller, and F. Stary, Nucl. Phys. **A370**, 47 (1981).
- <sup>32</sup>L. K. Peker, Nucl. Data Sheets (N.Y.) **43**, 579 (1984).
- <sup>33</sup>J. K. Tuli, Nucl. Data Sheets (N.Y.) **25**, 603 (1978).
- <sup>34</sup>J. K. Tuli, Nucl. Data Sheets (N.Y.) **27**, 97 (1979).
- <sup>35</sup>J. K. Tuli, Nucl. Data Sheets (N.Y.) **29**, 533 (1980).
- <sup>36</sup>L. K. Peker, Nucl. Data Sheets (N.Y.) **41**, 195 (1984).
- <sup>37</sup>B. Harmatz and W. B. Ewbank, Nucl. Data Sheets (N.Y.) **25**, 113 (1978).
- <sup>38</sup>L. K. Peker, Nucl. Data Sheets (N.Y.) **42**, 111 (1984).
- <sup>39</sup>K. S. Toth, Y. A. Ellis-Akovali, F. T. Avignone III, R. S. Moore, D. M. Moltz, J. N. Nitschke, P. A. Wilmarth, P. K. Lemmert, D. C. Sousa, and A. L. Goodman, Phys. Rev. C **32**, 342 (1985).
- <sup>40</sup>E. Nolte, G. Colombo, S. Z. Gui, G. Korschinek, W. Schollmeier, P. Kubik, S. Gustavsson, R. Geier, and H. Morinaga, Z. Phys. A **306**, 211 (1982).
- <sup>41</sup>G. Vanden Berghe, Z. Phys. **266**, 139 (1974).
- <sup>42</sup>V. Paar, Nucl. Phys. **A211**, 29 (1973).
- <sup>43</sup>A. Kuriyama, T. Marumori, K. Matsuyanagi, and R. Okamoto, Prog. Theor. Phys. Suppl. **58**, 103 (1975).
- <sup>44</sup>N. Freed and W. Miles, Nucl. Phys. **A158**, 230 (1970).
- <sup>45</sup>M. Waroquier and K. Heyde, Nucl. Phys. **A144**, 481 (1970).
- <sup>46</sup>B. H. Wildenthal, E. Newman, and R. L. Auble, Phys. Rev. C **3**, 1199 (1971).
- <sup>47</sup>L. K. Peker, Nucl. Data Sheets (N.Y.) **38**, 87 (1983).
- <sup>48</sup>J. Eisenberg and W. Greiner, *Nuclear Theory 3: Microscopic Theory of the Nucleus* (North-Holland, Amsterdam, 1972).
- <sup>49</sup>R. E. Laird, Phys. Rev. C **17**, 1498 (1978).
- <sup>50</sup>J. C. Hill and M. L. Wiedenbeck, Nucl. Phys. **A119**, 53 (1968).
- <sup>51</sup>R. F. Casten, Nucl. Phys. **A443**, 1 (1985).